INVESTIGATING THERMAL STABILITY IN HYDERABAD CITY, INDIA

SUBHANIL GUHA* AND HIMANSHU GOVIL

Department of Applied Geology, National Institute of Technology Raipur, Chhattisgarh, India
**Corresponding author email: subhanilguha@gmail.com*

Received: 2nd October 2024, **Accepted:** 25th November 2024

ABSTRACT

Thermal environment and land use status are the two controlling factors for determining the ecological health of any urban area. The study aims to investigates the stability of the relationship between land surface temperature with normalized difference built-up index in Hyderabad City, India using eight Landsat 8 data of the summer season in 2023. The study applies Pearson's method for determining the correlation coefficient of this relationship. The results represent a consistent nature of land surface temperature and normalized difference built-up index values in this summer season as the range of the mean (0.08 for normalized difference built-up index and 6.78 ºC for land surface temperature) and standard deviation (0.02 for normalized difference built-up index and 0.79 for land surface temperature) values of land surface temperature and normalized difference built-up index are significantly low. Land surface temperature and normalized difference built-up index values are very stable (correlation coefficient = > 0.63 for eight land surface temperature images and correlation coefficient = > 0.50 for eight normalized difference built-up index images). Moreover, normalized difference built-up index also built a stable strong positive relationship (average correlation coefficient =0.64) with land surface temperature. The summer season affects the vegetation life of the city and influences the relationship between land surface temperature and normalized difference built-up index. Built-up surface leads to an increase in the value of land surface temperature and also regulates the values of normalized difference built-up index. The study is useful for stable urban environmental planning.

Keywords: Landsat; Land surface temperature; Normalized difference built-up index; Urban Planning.

INTRODUCTION

The increasing worldwide pattern of urbanization and its impacts has led researchers to investigate the effects of human activity on the urban thermal environment, including Land Surface Temperature (LST) (Li *et al*., 2011; Liang *et al*., 2021). The average temperature in city areas was significantly higher than in the nearby rural areas (Khan *et al*., 2023). The conversion of vegetation and agricultural land into impermeable surfaces could decrease the quantity of surface moisture, change energy flow, and have an impact on the energy balance and thus, increasing the LST of a specific area (Jin *et al*., 2023; Ghanbari *et al*., 2023). Different LST result from variations in the Earth's surface illumination caused by irregular landscapes (Guha, 2021; Ullah *et al*., 2023). As urban areas expand, the land use/land cover

(LULC) changes, which affects the global climate, local ecosystems, and people's well-being (Rimal *et al*., 2019).

Thermal infrared bands (8-14μm wavelength) are used to calculate LST, which is valuable for environmental and climate change research in urban areas (Quattrochi & Luvall, 2014; Guha & Govil, 2021, 2022). Several studies have analysed the impact of landscape structure, built-up surface and the green area's pattern on the thermal environment in different cities (Dissanayake *et al*., 2019; Athukorala & Murayama, 2020; Song *et al*., 2020; Liu *et al*., 2022).

It is observed that normalized difference built-up index (NDBI) builds the strongest relationship with LST among all the LULC indices in any heterogeneous urban landscape (Guha *et al*., 2020, 2022). In summer, the weather is mostly dry and vegetation coverage is low. Hence, the relationship between LST and NDBI in summer is quite different from the other seasons.

Some research analyses are available on LST-related work in Hyderabad City. Suneetha & Reddy (2024) analysed LST variation in Hyderabad City due to the changes in vegetation and water coverage. Sreedhar & Bhole (2018) analysed seasonally Urban Heat Island in the Greater Hyderabad and observed that the nighttime LST variation is maximum during the summer season. Guha & Govil (2023) presented a stable relationship between LST and land use/land cover indices in Hyderabad City in the winter season using Landsat 8 data. In this study, eight Landsat 8 data (two each from March, April, May, and June in 2023) of Hyderabad City have been used. The main goals of the study are (i) to find out the consistency of LST and NDBI in Hyderabad city for the summer season and (ii) to analyse the strength of the LST-NDBI relationship in the summer months of a single year (2023). Armed with this information, we can pave the way for sustainable urban planning that accounts for seasonal changes and promotes a better quality of life for all.

MATERIAL AND METHODS

Study area

The research work was conducted in Hyderabad, the capital city of Telangana in South India, which is the sixth largest city in India. It is the largest and most-populous city of Telangana and is also considered the major urban hub for all of south-central interior India. Hyderabad is located between 17°12'01" N and 17°36'06" N and between 78°10'02" E and 78°39'02" E. It is a rolling upland and has an elevation of around 550 m (Fig. 1). It is located on the Musi River in the heart of the Telangana Plateau, a major upland region of the Indian peninsula. The city has many man-made lakes and is under a tropical savannah (Aw) climatic zone characterized by warm to hot monsoonal wet and dry seasons, with the periphery lands being characterized by a hot semi-arid climatic zone (BSh). The summer months (March, April, May, and June) are warm and humid. The average annual temperature and precipitation are 27 °C and 85 cm. Rainfall in the city are of moderate type and most rain falls during the wet monsoon months of June to October. The city has experienced high rates of urbanization in recent years.

Fig. 1: Location of the study area

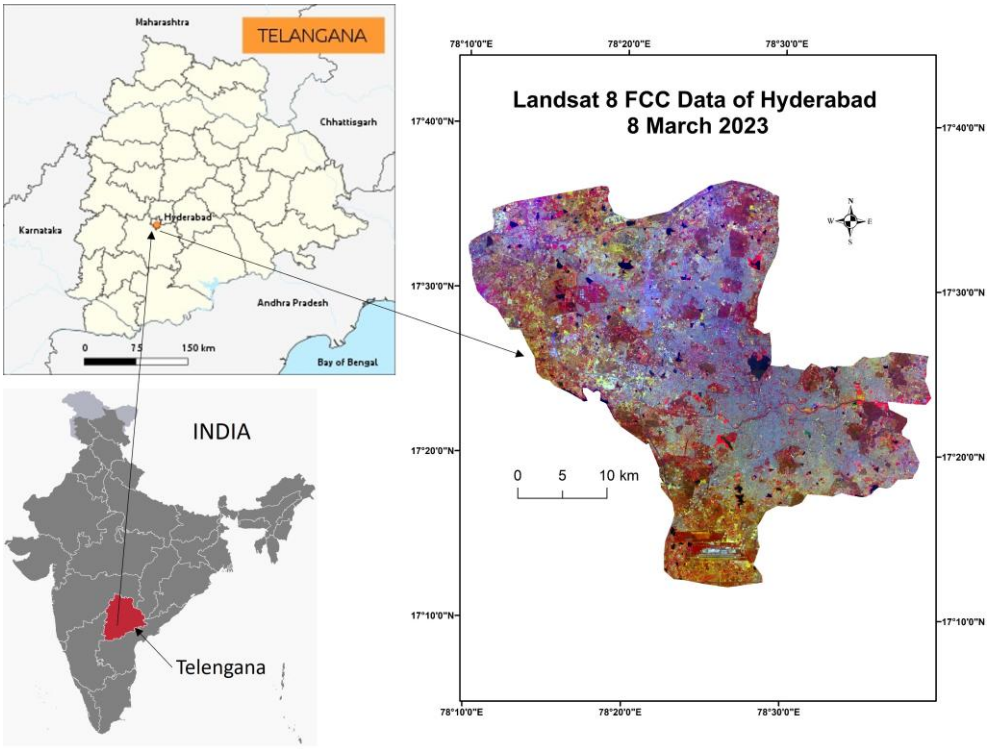

Data

The study utilized eight 2023 summer Landsat 8 satellite images of Hyderabad city, acquired from the United States Geological Survey (https://earthexplorer.usgs.gov/), which were taken on days with clear and dry weather (< 4% cloud coverage) (Table 1).

Table 1: Brief description of Landsat 8 data for the summer season in 2023

Landsat scene ID	Date of acquisition	Coordinated universal time (UTC)	Path/Row	Sun elevation (°)	Sun azimuth (°)	Cloud cover (%)	Earth-Sun distance (astronomical unit)
LC81440482020347LGN00	2023-03-08	05:09:39	144/048	55.16	127.48	0.37	0.99
LC81440482023083LGN00	2023-03-24	05:09:30	144/048	59.83	119.31	1.44	0.99
LC91440482023091LGN00	2023-04-01	05:09:38	144/048	62.01	114.51	0.87	0.99
LC81440482023099LGN00	2023-04-09	05:09:16	144/048	63.83	109.05	0.97	1.00
LC91440482023139LGN00	2023-05-19	05:09:14	144/048	67.52	80.24	0.55	1.01
LC81440482023147LGN00	2023-05-27	05:08:59	144/048	67.22	76.28	0.28	1.01
LC81440482023163LGN00	2023-06-12	05:09:07	144/048	66.39	71.74	3.16	1.01
LC91440482023171LGN00	2023-06-20	05:09:00	144/048	65.91	71.20	1.30	1.01

Table 2 shows the weather data (mean air temperature, rainfall, cloud cover, wind speed, etc.) of Hyderabad City for the summer season in 2023. The specific dates do not show any rainfall or significant cloud coverage. The wind speed varies from 9.25 kmph to 25.91 kmph during the acquisition time of satellite images. These weather data influence a lot on the LST of the study area. The air temperature differs from LST by a narrow range and generally, the air temperature should be slight lower than the LST in the summer season of humid tropical environment.

Table 2: Weather data of Hyderabad City for the summer season in 2023

Date	Mean Air Temperature (°C)	Rainfall (mm)	Cloud Cover (%)	Wind Speed (kmph)
2023-03-08	28.9	0	No significant cloud	9.25
2023-03-24	28.1	0	No significant cloud	14.82
2023-04-01	30.0	0	No significant cloud	11.10
2023-04-09	32.2	0	No significant cloud	11.10
2023-05-19	33.1	0	No significant cloud	9.25
2023-05-27	29.8	0	No significant cloud	11.10
2023-06-12	26.2	0	Mostly clear	25.91
2023-06-20	30.3	0	Mostly clear	11.10

METHODOLOGY

Determination of NDBI

NDBI is considered the most influential LULC index that builds the strongest relationship with LST in any season in an urban environment (Zha *et al*., 2003). However, NDBI is frequently used in extracting the built-up surface of mixed urban areas (Guha and Govil 2022; 2023). NDBI utilizes the Shortwave Infrared 1 (SWIR1) and NIR bands to determine its value. In Landsat 8 data, band 6 (SWR1) and band 5 (NIR) are used to obtain the NDBI value. A brief description of NDBI has been given in Table 3.

Table 3: A brief description of NDBI

Acronym	Description	Formulation	References
NDBI	Normalized difference built-up index	SWIR1-NIR/SWIR1+NIR	Zha *et al*. 2003

LST calculation

LST is calculated by using Landsat TIR band and the whole process follows some algorithms. First, spectral radiance is calculated by the following equation (Artis & Carnahan, 1982):

$$L_\lambda = RadianceMultiBand \times DN + RadianceAddBand \quad (1)$$

L_λ = the spectral radiance in $Wm^{-2}sr^{-1}mm^{-1}$.

Then, the at-sensor brightness temperature is calculated by the following equation:

$$T_B = \frac{K_2}{\ln((K_1 / L_\lambda) + 1)} \quad (2)$$

Where, T_B = brightness temperature in Kelvin (K), L_λ = spectral radiance in $Wm^{-2}sr^{-1}mm^{-1}$; K_2 and K_1 = calibration constants.

Then, fractional vegetation is calculated by the following equation (Carlson and Ripley 1997):

$$F_v = \left(\frac{NDVI - NDVI_{min}}{NDVI_{max} - NDVI_{min}} \right)^2 \quad (3)$$

Where, $NDVI_{min}$ = minimum NDVI, $NDVI_{max}$ = maximum NDVI. F_v = fractional vegetation.

Then, land surface emissivity ε, is calculated by the following equation (Sobrino et al. 2001, 2004):

$$\varepsilon = 0.004 * F_v + 0.986 \quad (4)$$

Where, ε = surface emissivity.

Lastly, LST is calculated by the following equation (Weng *et al*., 2004):

$$LST = \frac{T_B}{1 + (\lambda \sigma T_B / (hc)) \ln \varepsilon} \quad (5)$$

Where, λ = effective wavelength, σ = Boltzmann constant (1.38×10^{-23} J/K), h = Plank's constant (6.626×10^{-34} Js), c = velocity of light in a vacuum (2.998×10^{-8} m/sec), ε = emissivity. Fig. 2 shows the structure of the methodology of the entire work.

Fig. 2: Methodology of the study

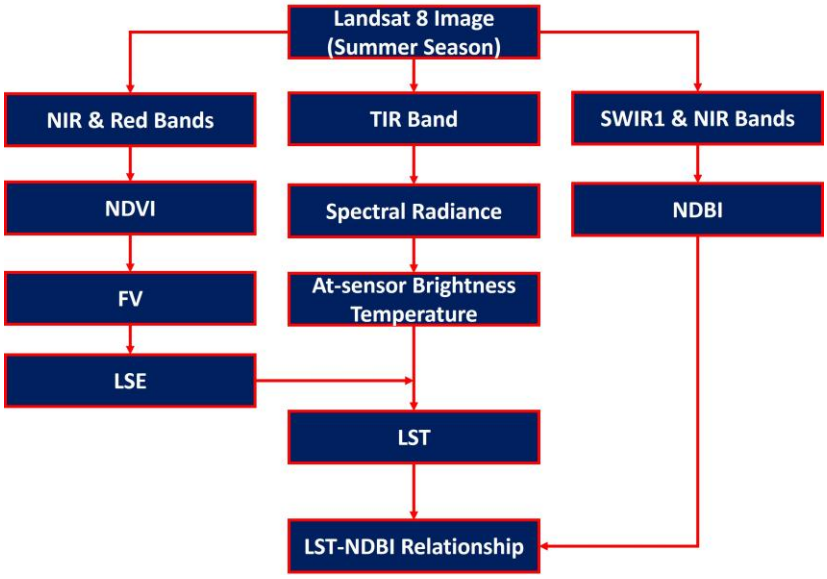

RESULTS

Spatial status of LST

During the summer season of 2023, there a noteworthy LST values which are shown in Fig. 3 and Fig. 4. Figure 3 uses separate LST legend for separate satellite image to show the actual distribution of LST. Figure 4 uses a single common LST legend for all eight satellite images to derive a better comparison. The mean, minimum and maximum LST remain stable due to consistent weather conditions and the use of the same season. All surface materials remain almost unchanged. In every image, the northwest and southeast periphery of the city have higher LST. However, the middle part of the city is less heated because of the concentration of water bodies and vegetation.

Fig. 3: LST distribution values using separate legends: (a) 8-Mar-2023 (b) 24-Mar-2023 (c) 1-Apr-2023 (d) 9-Apr-2023 (e) 19-May-2023 (f) 27-May-2023 (g) 12-Jun-2023 (h) 20-Jun-2023

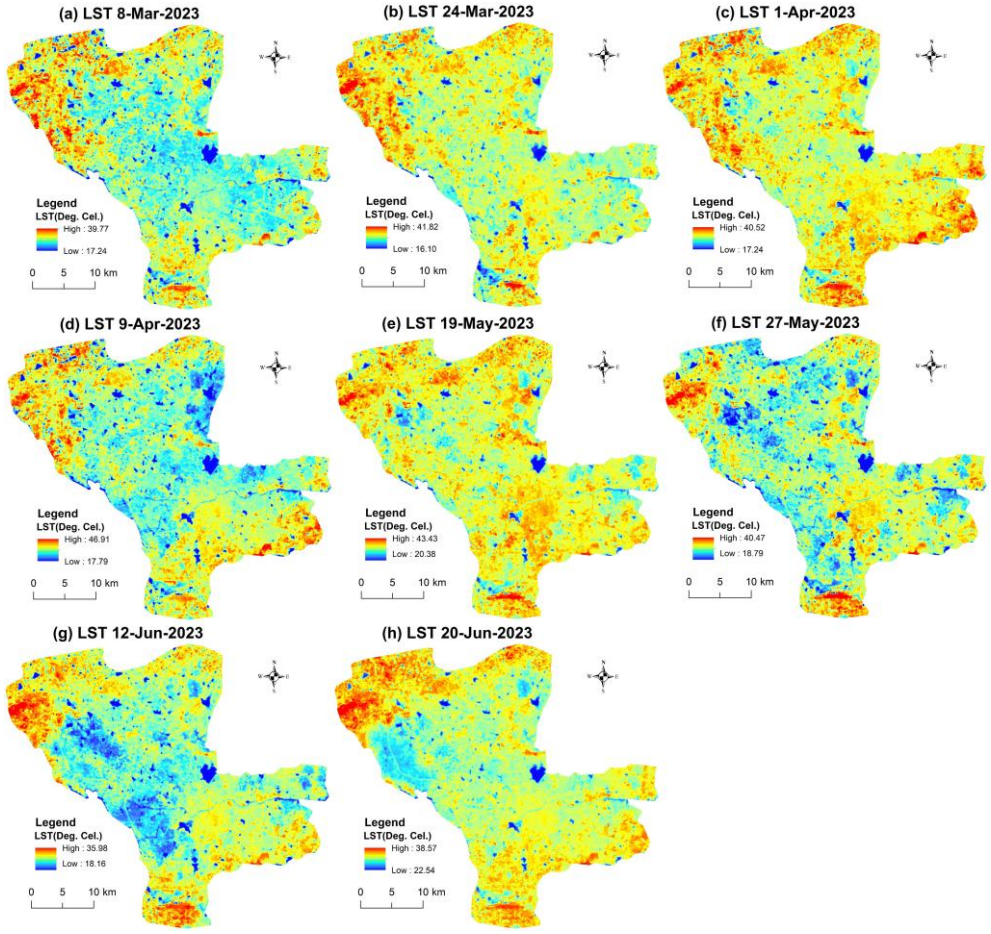

Fig. 4: LST distribution values using a single legend: (a) 8-Mar-2023 (b) 24-Mar-2023 (c) 1-Apr-2023 (d) 9-Apr-2023 (e) 19-May-2023 (f) 27-May-2023 (g) 12-Jun-2023 (h) 20-Jun-2023

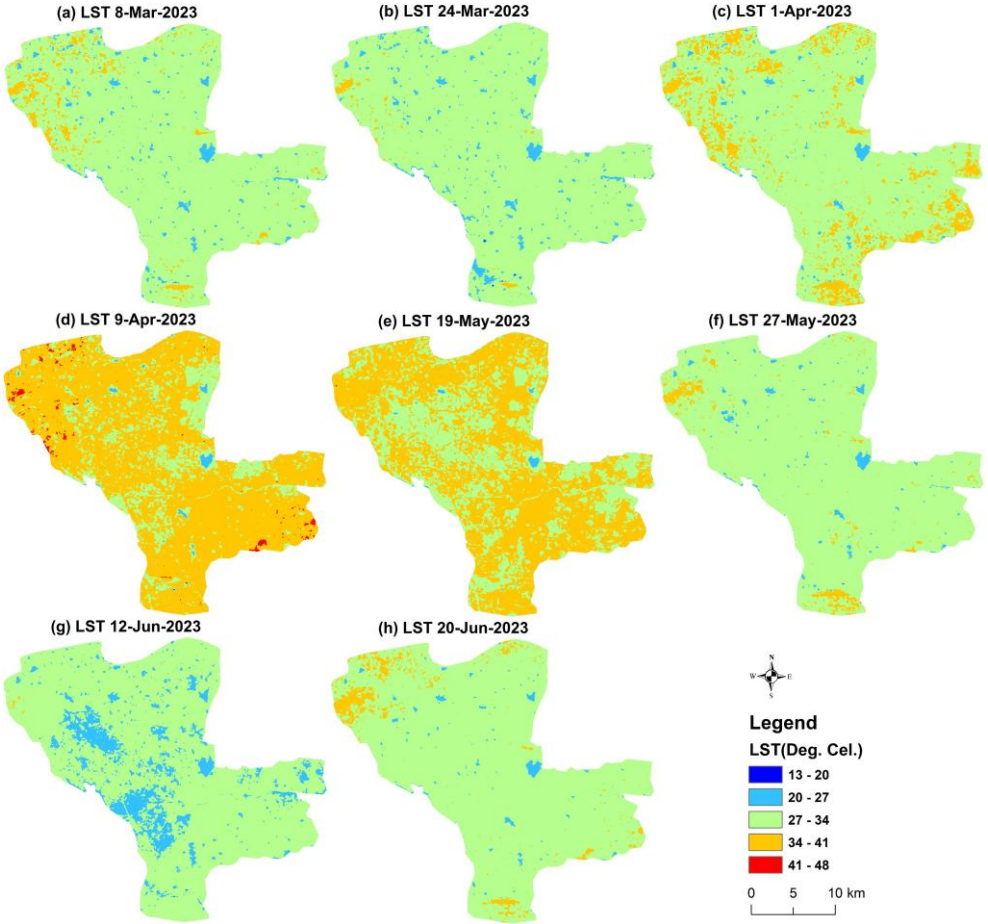

Table 4 displays the distribution of LST in Hyderabad City for eight images of the summer season. The minimum LST varies from 16.10°C (24 March) to 22.54°C (20 June), the maximum LST varies from 35.98°C (12 June) to 46.91°C (9 April), and the mean LST varies from 28.84°C (12 June) to 35.62°C (9 April). The statistics reveal that LST remained quite stable throughout the summer season. The narrow range of the minimum (6.44°C), maximum (10.93°C), and mean (6.76°C) LST for summer months indicates the high consistency of LST. The middle parts of the city indicate lower LST values compared to the periphery regions.

Table 3: A detailed description of LST and NDBI

	LST (ºC)				NDBI			
Date of acquisition	Min.	Max.	Mean	Std. Dev.	Min.	Max.	Mean	Std. Dev.
8-Mar	17.24	39.77	30.60	1.99	-0.38	0.48	0.01	0.06
24-Mar	16.10	41.82	29.91	1.69	-0.42	0.42	-0.01	0.07
1-Apr	17.24	40.52	32.21	1.89	-0.43	0.27	-0.01	0.07
9-Apr	17.79	46.91	35.62	2.43	-0.44	0.30	-0.02	0.07
19-May	20.38	43.43	34.27	1.81	-0.43	0.57	-0.06	0.07
27-May	18.79	40.47	31.19	1.64	-0.44	0.36	-0.07	0.07
12-Jun	18.16	35.98	28.84	1.73	-0.46	0.55	-0.05	0.07
20-Jun	22.54	38.58	31.23	1.67	-0.36	0.26	-0.05	0.05

Spatial status of NDBI

Fig. 5: NDBI distribution values using separate legends: (a) 8-Mar-2023 (b) 24-Mar-2023 (c) 1-Apr-2023 (d) 9-Apr-2023 (e) 19-May-2023 (f) 27-May-2023 (g) 12-Jun-2023 (h) 20-Jun-2023

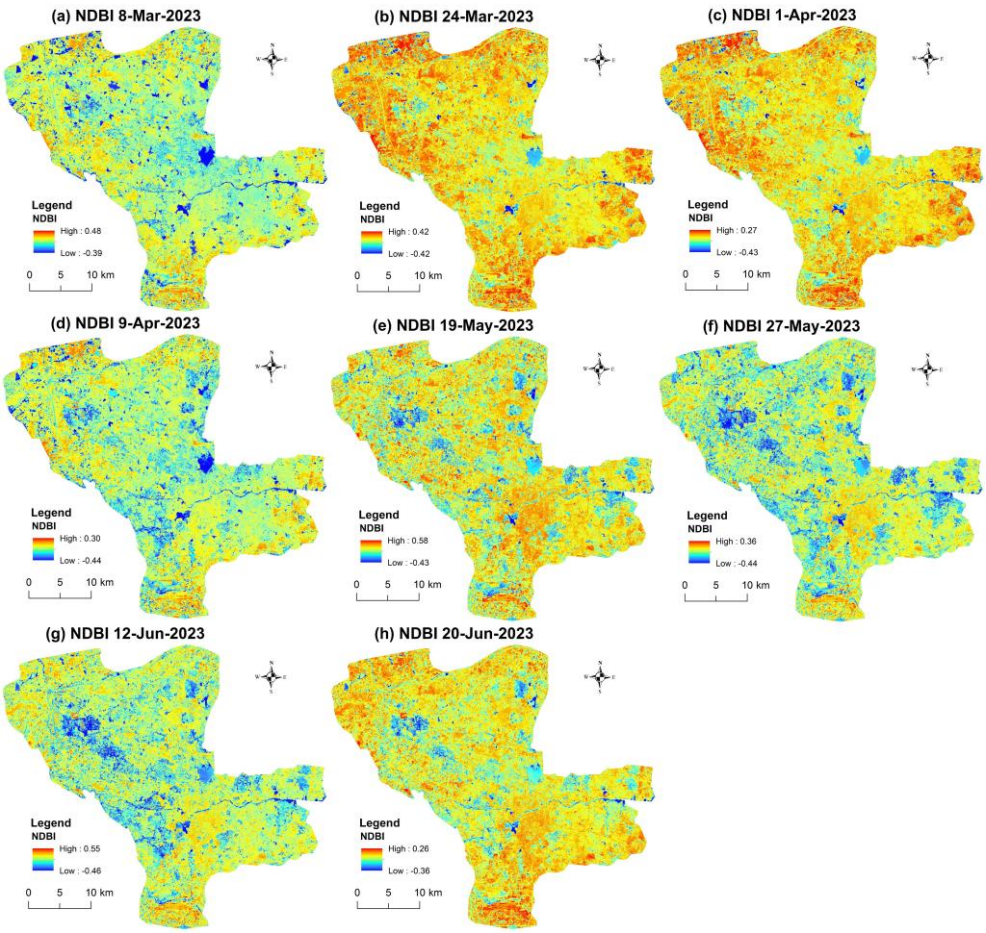

Figure 5 and 6 display the spatial distribution of NDBI values for the Landsat 8 images taken during the summer of 2023. Figure 5 uses separate legends for separate single satellite image to show the actual distribution of NDBI. Figure 6 uses a single common legend for all satellite images to derive a better comparison. The images show a stable view, indicating that the weather conditions and surface composition are almost unchanged. All the images produce almost the same NDBI values separately. However, the eastern and central parts have lower NDBI values while the northwest corner and southeast corners have higher NDBI. The spatial distribution of LST has a positive correlation with NDBI values.

Fig. 6: NDBI distribution values using a single legend: (a) 8-Mar-2023 (b) 24-Mar-2023 (c) 1-Apr-2023 (d) 9-Apr-2023 (e) 19-May-2023 (f) 27-May-2023 (g) 12-Jun-2023 (h) 20-Jun-2023

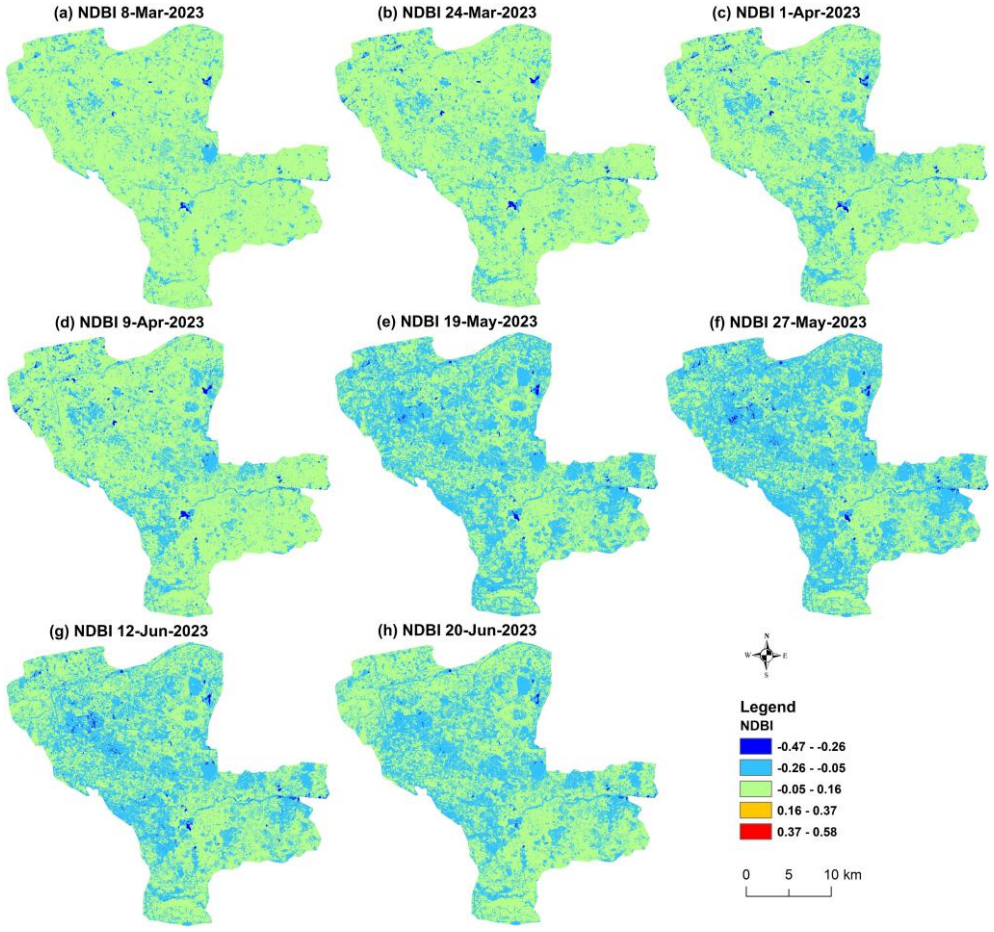

Table 4 also provides a detailed analysis of NDBI values for eights images of four summer months. The mean NDBI values have a narrow range (0.08), as do the minimum and maximum NDBI values (0.10 and 0.29, respectively). Additionally, the standard deviation of NDBI values is quite low (0.01), which indicates stable surface characteristics and consistent weather conditions. The results for April, May, and June are particularly consistent.

DISCUSSION

Correlation status between LST and NDBI

Table 5 represents the correlation matrices of NDBI and LST. LST of April is very strongly correlated to March (0.85), and strongly correlated to May (0.74), and June (0.78). LST of March is also strongly correlated to May (0.63), and June (0.70). The LST of May is very strongly correlated to the LST of June (0.80). For NDBI, April is very strongly correlated to March (0.85), and strongly correlated to May (0.65), and June (0.71). NDBI of March is moderately correlated to May (0.50) and June (0.59). However, the NDBI of May is very strongly correlated to the NDBI of June (0.92). In the correlation matrix table, the correlation coefficient values of > 0.8 have been highlighted by grey colour.

Table 5: Correlation matrices of LST and NDBI

Correlation matrix of LST								
Date of acquisition	8-Mar	24-Mar	1-Apr	9-Apr	19-May	27-May	12-Jun	20-Jun
8-Mar	1.00000							
24-Mar	0.86367	1.00000						
1-Apr	0.86135	0.85755	1.00000					
9-Apr	0.85302	0.84264	0.92716	1.00000				
19-May	0.69284	0.77543	0.83725	0.77261	1.00000			
27-May	0.63185	0.73128	0.80432	0.74181	0.90965	1.00000		
12-Jun	0.70215	0.71248	0.76066	0.78033	0.78861	0.79916	1.00000	
20-Jun	0.68903	0.66758	0.73684	0.75425	0.78908	0.74787	0.86319	1.00000
Correlation matrix of NDBI								
Date of acquisition	8-Mar	24-Mar	1-Apr	9-Apr	19-May	27-May	12-Jun	20-Jun
8-Mar	1.00000							
24-Mar	0.91978	1.00000						
1-Apr	0.87391	0.92966	1.00000					
9-Apr	0.85068	0.90811	0.95672	1.00000				
19-May	0.55910	0.58191	0.68110	0.69305	1.00000			
27-May	0.50028	0.53278	0.63548	0.65009	0.94700	1.00000		
12-Jun	0.58705	0.61973	0.69075	0.70832	0.88265	0.91778	1.00000	
20-Jun	0.65098	0.66494	0.71911	0.72833	0.85798	0.86209	0.94711	1.00000

Table 6: Correlation coefficients (*r*) of LST-NDBI correlation analyses

Date of acquisition	LST-NDBI
8-Mar-2023	0.66188
24-Mar-2023	0.59108
1-Apr-2023	0.68212
9-Apr-2023	0.65515
19-May-2023	0.66552
27-May-2023	0.65440
12-Jun-2023	0.57649
20-Jun-2023	0.59524
Average	0.635235

Table 6 represents the correlation coefficients of LST-NDBI relationships. The March images (0.66 and 0.59), April images (0.68 and 0.66), and May images (0.67 and 0.65) reflect almost equal strength of correlation. The Correlation coefficient value for the June image is slightly lower (0.58 and 0.60). However, the average correlation coefficient value for the eight summer images is 0.64. It indicates a strong correlation between LST and NDBI for the summer of 2023 in Hyderabad city.

The LST-NDBI relationship noticed in the summer months is consistently stable (range = 0.1) and strongly positive (the average r = 0.64). This result is closely comparable to some LST-NDBI-related studies conducted in Fuzhou (Zhang *et al*., 2009), Bahir Dar (Balew & Korme, 2020), Melbourne (Jamei *et al*. 2019), San Salvador (Son *et al*., 2020), Kunming (Chen & Zhang, 2017), Lagos (Alademomi *et al*., 2022), Varanasi (Tiwari & Kanchan, 2024), Kayseri (Cetin *et al.*, 2024), Vellore (Manjunath & Jagadeesh), etc. The Pearson's correlation coefficient in four seasons for Wuhan City, China was 0.639, 0.717, 0.807 and 0.762 respectively (Chen *et al*., 2013) which is comparable with the present research outcome. Kumar *et al*. (2023) tried to identify the climatic change and the thermal Comfort Zones with the use of the LST and NDBI in Andhra Pradesh, South India's semi-arid regions. Biney *et al*. (2024) analyzed the spatio-temporal pattern of urban growth and its influence on urban heat islands in the Sekondi-Takoradi metropolis, Ghana by using LST-NDBI relationship. Santosh & Shilpa (2023) established a significant relationship between LST and NDBI along with other LULC indices on different LULC types in Bengaluru district, India. Another significant study on Granada (Spain) showed the effective correlation between LST and NDBI in modelling the surface urban heat islands (Hidalgo-García & Arco-Díaz. 2022). Zhao et al. (2024) evaluated the LULC changes with respect to LST and found a strong positive relation of LST with NDBI in Kasur district, Pakistan. Fu *et al.* (2024) predicted the surface urban heat islands for LST and NDBI because of their strong correlation coefficient value.

CONCLUSION

The paper assesses the stability of the spatial correlation between land surface temperature and normalized difference built-up index using eight Landsat 8 data of the 2023 summer season in Hyderabad city. Land surface temperature and normalized difference built-up index have maintained a substantially stable value throughout the period, and also exhibit a consistent relationship during the summer season because of the marginal changes in weather and land surface conditions. The peripheral areas of the city have experienced relatively high land surface temperature and normalized difference built-up index values. Normalized difference built-up index and land surface temperature show a strong positive correlation during the three summer months (March (0.63), April (0.67), and May (0.66)) and a moderate positive correlation in June (0.59). Among all four months, April is considered the most reliable in terms of consistency.

ACKNOWLEDGMENT

The authors are indebted to United States Geological Survey (USGS).

CONFLICTS OF INTEREST

The authors declare no conflict of interest

REFERENCES

Alademomi, A.S., Okolie, C.J., Daramola, O.E., Akinnusi, S.A., Adediran, E., Olanrewaju, H.O., Alabi, A.O., Salami, T.J., Odumosu, J. (2022). The interrelationship between LST, NDVI, NDBI, and land cover change in a section of Lagos metropolis, Nigeria. *Appl Geomat* 14, 299–314. https://doi.org/10.1007/s12518-022-00434-2

Artis, D.A., Carnahan, W.H. (1982). Survey of emissivity variability in thermography of urban areas. *Remote Sens Environ* 12(4): 313–329.

Athukorala, D., Murayama, Y. (2020). Spatial variation of land use/cover composition and impact on surface urban heat island in a tropical sub-Saharan City of Accra, Ghana. *Sustainability* 12(19). https://doi.org/10.3390/SU12197953

Balew, A., Korme, T., (2020). Monitoring land surface temperature in Bahir Dar city and its surroundings using Landsat images. *Egypt J Remote Sens Space Sci* https://doi.org/10.1016/j.ejrs.2020.02.001

Biney, E., Forkuo, E.K., Poku-Boansi, M,. Hackman, K.O., Harris, E., Asare, Y.M., Yankey, D.B., Annan, E., Agbenorhevi, A.E. (2024). Analyzing the spatio-temporal pattern of urban growth and its influence on urban heat islands in the Sekondi-Takoradi metropolis. Ghana. *Sci Afr* 26: e02366. https://doi.org/10.1016/j.sciaf.2024.e02366

Carlson, T.N., Ripley, D.A. (1997). On the Relation between NDVI, Fractional Vegetation Cover, and Leaf Area Index. *Remote Sens Environ* 62: 241-252. https://doi.org/10.1016/S0034-4257(97)00104-1

Cetin, M., Ozenen Kavlak, M., Senyel Kurkcuoglu, M.A., Bilge Ozturk, G., Nihan Cabuk, S., Cabuk, A. (2024). Determination of land surface temperature and urban heat island effects with remote sensing capabilities: the case of Kayseri, Türkiye. *Nat Hazards* 120, 5509–5536 (2024). https://doi.org/10.1007/s11069-024-06431-5

Chen, L., Li, M., Huang, F., Xu, S. (2013). Relationships of LST to NDBI and NDVI in Wuhan City based on Landsat ETM+ image. *2013 6th International Congress on Image and Signal Processing (CISP)*, Hangzhou, 2013, pp. 840-845.

Chen, X.L., Zhao, H.M., Li, P.X., Yi, Z.Y. (2006). Remote sensing image-based analysis of the relationship between urban heat island and land use/cover changes. *Remote Sens Environ* 104(2): 133–146. https://doi.org/10.1016/j.rse.2005.11.016

Chen, X., Zhang, Y. (2017). Impacts of urban surface characteristics on spatiotemporal pattern of land surface temperature in Kunming of China. *Sustain Cities Soc.* 32: 87-99. https://doi.org/10.1016/j.scs.2017.03.013

Dissanayake, DMSLB, Morimoto, T., Murayama, Y., Ranagalage, M., (2019). Impact of landscape structure on the variation of land surface temperature in Sub-Saharan Region: A case study of Addis Ababa using Landsat Data (1986 -2016). *Sustainability* 11(8). https://doi.org/10.3390/su11082257

Fu, S., Wang, L., Khalil, U., Cheema, A.H., Ullah, I., Aslam, B., Tariq, A., Aslam, M., Alarifi, S.S. (2024). Prediction of surface urban heat island based on predicted consequences of urban sprawl using deep learning: A way forward for a sustainable environment. *Phys Chem Earth Parts A/B/C* 35: 103682. https://doi.org/10.1016/j.pce.2024.103682

Ghanbari, R., Heidarimozaffar, M., Soltani, A., Arefi, H. (2023). Land surface temperature analysis in densely populated zones from the perspective of spectral indices and urban morphology. *Int J Environ Sci Tech* 20:2883–2902. https://doi.org/10.1007/S13762-022-04725-4

Guha, S., Govil, H. (2023). Evaluating the stability of the relationship between land surface temperature and land use/land cover indices: a case study in Hyderabad city, India. *Geol Ecol Landsc* 1–13. https://doi.org/10.1080/24749508.2023.2182083

Guha, S., Govil, H. (2022). Annual assessment on the relationship between land surface temperature and six remote sensing indices using Landsat data from 1988 to 2019. *Geocarto Int* 37(15): 4292-4311. https://doi.org/10.1080/10106049.2021.1886339

Guha, S. (2021). Dynamic seasonal analysis on LST-NDVI relationship and ecological health of Raipur City, India. *Ecosyst Health Sust* 7(1): 1927852. https://doi.org/10.1080/20964129.2021.1927852

Guha, S., Govil, H. (2021). A long-term monthly analytical study on the relationship of LST with normalized difference spectral indices. *Eur J Remote Sens* 54(1): 487-512. https://doi.org/10.1080/22797254.2021.1965496

Guha, S., Govil, H., Gill, N., Dey, A. (2020). A long-term seasonal analysis on the relationship between LST and NDBI using Landsat data. *Quatern Int* https://doi.org/10.1016/j.quaint.2020.06.041

Guha, S., Govil, H., Taloor, A.K., Gill, N., Dey, A. (2022). Land surface temperature and spectral indices: A seasonal study of Raipur City. *Geod Geodyn* 13(1): 72-82. https://doi.org/10.1016/j.geog.2021.05.002

Hidalgo-García, D., Arco-Díaz, J. (2022). Modeling the Surface Urban Heat Island (SUHI) to study of its relationship with variations in the thermal field and with the indices of land use in the metropolitan area of Granada (Spain). *Sustain Cities Soc* 87: 104166. https://doi.org/10.1016/j.scs.2022.104166 , http://earthexplorer.usgs.gov/

Jamei, Y., Rajagopalan, P., Sun, Q.C. (2019). Spatial structure of surface urban heat island and its relationship with vegetation and built-up areas in Melbourne, Australia. *Sci Total Environ* 659: 1335-1351. https://doi.org/10.1016/j.scitotenv.2018.12.308

Jin, K., Qin, M., Tang, R., Huang, X., Hao, L., Sun, G. (2023). Urban-rural interface dominates the effects of urbanization on watershed energy and water balances in Southern China. *Landsc Ecol*. https://doi.org/10.1007/S10980-023-01648-4

Khan, M., Qasim, M., Tahir, A.A., Farooqi, A. (2023). Machine learning-based assessment and simulation of land use modification effects on seasonal and annual land surface temperature variations. *Heliyon* 9:e23043. https://doi.org/10.1016/j.heliyon.2023.e23043

Kumar, B.P., Anusha, B.N., Raghu Babu, K., Padma Sree, P. (2023). Identification of climate change impact and thermal comfort zones in semi-arid regions of AP, India using LST and NDBI techniques. *J Cleaner Prod* 407: 137175.https://doi.org/10.1016/j.jclepro.2023.137175

Li, J., Song C, Cao L, Meng X, Wu J (2011). Impacts of landscape structure on surface urban heat islands: A case study of Shanghai, China. *Remote Sens Environ* 115: 3249–3263.

Liang, X., Ji, X., Guo, N., Meng, L., (2021). Assessment of urban heat islands for land use based on urban planning: a case study in the main urban area of Xuzhou City, China. *Environ Earth Sci* 80. https://doi.org/10.1007/S12665-021-09588-5

Liu, S., Li, X., Chen, L., Zhao, Q., Zhao, C., Hu, X., Li, J. (2022). A New Approach to Investigate the Spatially Heterogeneous Cooling Effects of Landscape Pattern. *Land* 11(2). https://doi.org/10.3390/land11020239

Manjunath, D.R., Jagadeesh, P. (2024). Dynamics of urban development patterns on thermal distributions and their implications on water spread areas of Vellore, Tamil Nadu, India. *Front Sustain Cities* 6:1462092. https://doi.org/10.3389/frsc.2024.1462092

Quattrochi, D.A., Luvall, J.C. (2014). Thermal Infrared Remote Sensing For Analysis of Landscape Ecological Processes: Current Insights and Trends. *Scale Issues in Remote Sensing*, 9781118305041, 34–60. https://doi.org/10.1002/9781118801628.CH03

Rimal, B., Sharma, R., Kunwar, R., Keshtkar, H., Stork, N.E., Rijal, S., Rahman, S.A., Baral, H. (2019). Effects of land use and land cover change on ecosystem services in the Koshi River Basin, Eastern Nepal. *Ecosyst Serv* 38: 100963. https://doi.org/10.1016/J.ECOSER.2019.100963

Santhosh, L.G., Shilpa, D.N. (2023). Assessment of LULC change dynamics and its relationship with LST and spectral indices in a rural area of Bengaluru district, Karnataka India. *Remote Sens Appl Soc Environ* 29: 100886. https://doi.org/10.1016/j.rsase.2022.100886

Senanayake, I.P., Welivitiya, WDDP, Nadeeka, P.M. (2013). Remote sensing-based analysis of urban heat islands with vegetation cover in Colombo city, Sri Lanka using Landsat-7 ETM+ data. *Urban Clim* 5: 19–35. https://doi.org/10.1016/J.UCLIM.2013.07.004

Sobrino, J.A., Raissouni, N., Li, Z. (2001). A comparative study of land surface emissivity retrieval from NOAA data. *Remote Sens Environ* 75(2): 256–266. https://doi.org/10.1016/S0034-4257(00)00171-1

Sobrino, J.A., Jimenez-Munoz, J.C., Paolini, L. (2004). Land surface temperature retrieval from Landsat TM5. Remote Sens Environ 9: 434–440. https://doi:10.1016/j.rse.2004.02.003

Son, N.T., Chen, C.F., Chen, C.R. (2020). Urban expansion and its impacts on the local temperature in San Salvador, El Salvador. *Urban Clim* 32: 100617. https://doi.org/10.1016/j.uclim.2020.100617

Song, Y., Song, X., Shao, G. (2020). Effects of green space patterns on the urban thermal environment at multiple spatial -temp. *Sustainability* 12(17). https://doi.org/10.3390/S

Sridhar, N., Bhole, V. (2018). Seasonal Analysis of Urban Heat Island of Greater Hyderabad Using Thermal Remote Sensing. *J Remote Sens GIS* 9(1): 49–56.

Suneetha, Y., Reddy, M.A. (2024). Spatial and Temporal analysis of Landsat data to Retrieve the NDWI, NDVI and Land Surface Temperature by thermal remote sensor: A case study of Hyderabad Metropolitan City, Telangana. *E3S Web Conf.*, 472: 02003. https://doi.org/10.1051/e3sconf/202447202003

Tiwari, A.K., Kanchan, R. (2024). Analytical study on the relationship among land surface temperature, land use/land cover and spectral indices using geospatial techniques. *Discov Environ* 2, 1 (2024). https://doi.org/10.1007/s44274-023-00021-1

Ullah, W., Ahmad, K., Ullah, S., Tahir, A.A., Javed, M.F., Nazir, A., Abbasi, A.M., Aziz, M., Mohamed, A. (2023). Analysis of the relationship among land surface temperature (LST), land use land cover (LULC), and normalized difference vegetation index (NDVI) with topographic elements in the lower Himalayan region. *Heliyon* 9:e13322. https://doi.org/10.1016/j.heliyon.2023.e13322

Weng, Q.H., Lu, D.S., Schubring, J. (2004). Estimation of Land Surface Temperature–Vegetation Abundance Relationship for Urban Heat Island Studies. *Remote Sens Environ* 89: 467-483. https://doi:10.1016/j.rse.2003.11.005

Zhang, Y., Odeh, I.O.A., Han, C. (2009). Bi-temporal characterization of land surface temperature in relation to impervious surface area, NDVI and NDBI, using a sub-pixel image analysis. *Int J Appl Earth Obs Geoinf* 11(4): 256-264. https://doi.org/10.1016/j.jag.2009.03.001

Zhao, Q., Haseeb, M., Wang, X., Zheng, X., Tahir, Z., Ghafoor, S., Mubbin, M., Kumar,

R.P., Purohit, S., Soufan, W., Almutairi, K.F. (2024). Evaluation of Land Use Land Cover Changes in Response to Land Surface Temperature With Satellite Indices and Remote Sensing Data. *Rangeland Ecol Manag* 96: 183-196. https://doi.org/10.1016/j.rama.2024.07.003

Zha, Y., Gao, J., Ni, S. (2003). Use of normalized difference built-up index in automatically mapping urban areas from TM imagery. *Int J Remote Sens* 24(3): 583-594. https://doi.org/10.1080/01431160304987